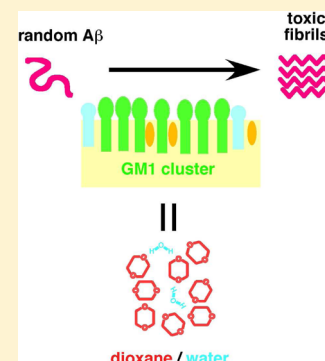


# GM1 Cluster Mediates Formation of Toxic A $\beta$ Fibrils by Providing Hydrophobic Environments

Saori Fukunaga, Hiroshi Ueno, Takahiro Yamaguchi, Yoshiaki Yano, Masaru Hoshino, and Katsumi Matsuzaki\*

Graduate School of Pharmaceutical Sciences, Kyoto University, 46-29 Yoshida-Shimoadachi-cho, Sakyo-ku, Kyoto 606-8501, Japan

**ABSTRACT:** The conversion of soluble, nontoxic amyloid  $\beta$ -proteins (A $\beta$ ) to aggregated, toxic forms rich in  $\beta$ -sheets is considered to be a key step in the development of Alzheimer's disease. Accumulating evidence suggests that lipid–protein interactions play a crucial role in the aggregation of amyloidogenic proteins like A $\beta$ . Our group has previously reported that amyloid fibrils of A $\beta$  formed on membranes containing clusters of GM1 ganglioside (M-fibrils) exhibit greater cytotoxicity than fibrils formed in aqueous solution (W-fibrils) [Okada et al. (2008) *J. Mol. Biol.* 382, 1066–1074]. W-fibrils are considered to consist of in-register parallel  $\beta$ -sheets. However, the precise molecular structure of M-fibrils and force driving the formation of toxic fibrils remain unclear. In this study, we hypothesized that low-polarity environments provided by GM1 clusters drive the formation of toxic fibrils and compared the structure and cytotoxicity of W-fibrils, M-fibrils, and aggregates formed in a low-polarity solution mimicking membrane environments. First, we determined solvent conditions which mimic the polarity of raftlike membranes using A $\beta$ -(1–40) labeled with the 7-diethylaminocoumarin-3-carboxyl dye. The polarity of a mixture of 80% 1,4-dioxane and 20% water (v/v) was found to be close to that of raftlike membranes. A $\beta$ -(1–40) formed amyloid fibrils within several hours in 80% dioxane (D-fibrils) or in the presence of raftlike membranes, whereas a much longer incubation time was required for fibril formation in a conventional buffer. D-fibrils were morphologically similar to M-fibrils. Fourier-transform infrared spectroscopy suggested that M-fibrils and D-fibrils contained antiparallel  $\beta$ -sheets. These fibrils had greater surface hydrophobicity and exhibited significant toxicity against human neuroblastoma SH-SY5Y cells, whereas W-fibrils with less surface hydrophobicity were not cytotoxic. We concluded that ganglioside clusters mediate the formation of toxic amyloid fibrils of A $\beta$  with an antiparallel  $\beta$ -sheet structure by providing less polar environments.



It is widely accepted that the conversion of the soluble, nontoxic amyloid  $\beta$ -protein (A $\beta$ ) monomer to aggregated toxic A $\beta$  rich in  $\beta$ -sheet structures is central to the development of Alzheimer's disease, a progressive neurodegenerative disorder.<sup>1,2</sup> However, the mechanism of the abnormal aggregation of A $\beta$  in vivo is not well understood. We have proposed that ganglioside clusters in lipid raft microdomains on neuronal cells play a crucial role in the formation of amyloid fibrils by A $\beta$ .<sup>3,4</sup> GM1 is an acidic glycosphingolipid abundant in plasma membranes of neurons and has been considered to be involved in the pathology of AD.<sup>4–6</sup> A $\beta$  recognizes and binds to a GM1 cluster,<sup>7</sup> changing its conformation from a random coil to an  $\alpha$ -helix-rich structure at lower protein densities on the membrane (A $\beta$ /GM1 <  $\sim$ 0.013) and a  $\beta$ -sheet-aggregate coexists at intermediate protein densities ( $\sim$ 0.013 < A $\beta$ /GM1 <  $\sim$ 0.044). At A $\beta$ /GM1 values above  $\sim$ 0.044, the  $\beta$ -structure is converted to a second, seed-prone  $\beta$ -structure. The seed recruits monomers from the aqueous phase to form amyloid fibrils.<sup>8</sup> Notably, amyloid fibrils formed in membranes (M-fibrils) are cytotoxic, whereas those formed in aqueous solution (W-fibrils) are not.<sup>9</sup> W-fibrils are considered to consist of in-register parallel  $\beta$ -sheets.<sup>10,11</sup> In contrast, the precise molecular structure of M-fibrils and the reasons why toxic fibrils are formed in membranes remain unclear.

In this paper, we hypothesized that low-polarity environments provided by GM1 clusters drive the formation of toxic

fibrils because polarity modulates both electrostatic and hydrophobic interactions that determine the structure of amyloid fibrils. To mimic such microenvironments, we used a mixture of 1,4-dioxane and phosphate-buffered saline (PBS) because (1) the organic solvent is freely miscible with water, therefore the same stock solution of A $\beta$  can be used to prepare both types of fibrils, and (2) the presence of CH<sub>2</sub>, ether O, and OH groups chemically mimics the sugar group of GM1. We found that the mixture facilitated the formation of A $\beta$  fibrils with a similar morphology, secondary structure, surface hydrophobicity, and cytotoxicity to M-fibrils. The mechanisms by which low-polarity environments drive the formation of amyloid fibrils with distinct properties will be discussed.

## MATERIALS AND METHODS

**A $\beta$ .** A $\beta$ -(1–40) was produced as an ubiquitin extension<sup>12</sup> and purified as described in detail elsewhere.<sup>13</sup> The protein was dissolved in 0.02% ammonia on ice, and any large aggregates which may act as a seed for aggregation were removed by ultracentrifugation in 500  $\mu$ L polyallomer tubes at 540000g, 4  $^{\circ}$ C for 3 h. The protein concentration of the supernatant was

**Received:** June 22, 2012

**Revised:** September 25, 2012

**Published:** September 25, 2012



determined in triplicate by the Micro BCA protein assay (Pierce, Rockford, IL). The supernatant was collected and stored at  $-80^{\circ}\text{C}$  prior to use. Just before the experiment, the stock solution was mixed with an equal volume of double concentrated PBS (NaCl 16.0 g/L, KCl 0.40 g/L,  $\text{Na}_2\text{HPO}_4$  2.3 g/L,  $\text{KH}_2\text{PO}_4$  0.4 g/L, pH 7.4).  $\text{A}\beta$ -(1–40) assumes a monomeric state under these conditions.<sup>14</sup>

**Small Unilamellar Vesicles (SUVs).** GM1 from bovine brain was purchased from Larodan (Malmö, Sweden). Cholesterol and *N*-acyl-D-sphingosine-1-phosphocholine from bovine brain (SM) were obtained from Sigma (St. Louis, MO). SUVs were prepared as described previously.<sup>7,15</sup> GM1, cholesterol, and SM were dissolved in a chloroform–methanol 1:1 (v/v) mixture, ethanol, and chloroform, respectively. The concentrations of GM1, cholesterol, and SM were determined at least in triplicate by the resorcinol–hydrochloric acid method,<sup>16</sup> the cholesterol oxidase method (free cholesterol E-test kit by Wako (Osaka, Japan)), and the phosphorus assay,<sup>17</sup> respectively. GM1, cholesterol, and SM were mixed at a molar ratio of 4:3:3, and the solvent was removed by evaporation in a rotary evaporator. The residual lipid film, after drying under vacuum overnight, was hydrated with PBS. The hydrated film was vortex mixed to produce multilamellar vesicles, which were subsequently sonicated under a nitrogen atmosphere for 9 min (3 min  $\times$  3 times) using a probe-type sonicator Tomy UD-201 (Tokyo, Japan). Metal debris from the titanium tip of the probe was removed by centrifugation. The concentration of vesicles was determined based on the concentration of GM1.<sup>18</sup> The vesicles have been characterized in terms of size and lamellarity.<sup>19</sup>

**Estimation of Polarity around  $\text{A}\beta$ .**  $\text{A}\beta$ -(1–40) labeled with the 7-diethylaminocoumarin-3-carbonyl group at its N-terminus (DAC- $\text{A}\beta$ -(1–40)) was custom synthesized and characterized by Peptide Institute (Minoh, Japan).<sup>7</sup> The dye-labeled peptide was always handled in light-protected, capped tubes under a nitrogen atmosphere to avoid photodegradation. Fluorescence spectra of 0.5  $\mu\text{M}$  DAC- $\text{A}\beta$ -(1–40) were measured in various 1,4-dioxane–PBS mixtures (open circles) as well as in the presence of raftlike SUVs composed of GM1/cholesterol/SM (4:3:3) ([GM1] = 50  $\mu\text{M}$ ) at  $37^{\circ}\text{C}$  at an excitation wavelength of 415 nm on a Shimadzu RF-5300 spectrofluorometer (Kyoto, Japan). Blank spectra (solvent or SUVs) were subtracted. Highly purified dioxane (>99.7%, Wako, Osaka Japan) was used to avoid the oxidation of the protein. The salt concentrations were kept constant in all samples by use of differently concentrated PBS solutions.

**Amyloidogenesis.** 50  $\mu\text{M}$   $\text{A}\beta$ -(1–40) was incubated in PBS, 1,4-dioxane/5xPBS (80:20, v/v), and raftlike SUVs composed of GM1/cholesterol/SM (4:3:3) ([GM1] = 50  $\mu\text{M}$ ) at  $37^{\circ}\text{C}$  under an argon atmosphere to avoid oxidation. Amyloid formation by  $\text{A}\beta$ -(1–40) was monitored by the thioflavin T (Th-T) assay. The sample (final  $\text{A}\beta$  concentration, 0.5  $\mu\text{M}$ ) was added to a 5  $\mu\text{M}$  ThT solution in 50 mM glycine buffer (pH 8.5). Fluorescence at 490 nm was measured at an excitation wavelength of 446 nm at  $25^{\circ}\text{C}$ .<sup>20,21</sup> The blank fluorescence (solvent or SUVs) was subtracted.

**CD Spectra.** The CD spectrum of 15  $\mu\text{M}$   $\text{A}\beta$ -(1–40) in 1,4-dioxane/5xPBS (80:20, v/v) was measured on a Jasco J-820 apparatus at  $15^{\circ}\text{C}$  to avoid aggregation of the protein. A 1 mm path length quartz cell was used to minimize the absorbance due to buffer components. The instrumental outputs were calibrated with nonhygroscopic ammonium *d*-camphor-10-

sulfonate.<sup>22</sup> Eight scans were averaged for each sample. The blank spectrum (solvent) was subtracted.

**Preparation of Various Fibrils.** Amyloid fibrils were prepared in PBS (W-fibrils), 20% 1,4-dioxane/80% 1.25xPBS (v/v, D<sub>20</sub>-fibrils), 80% 1,4-dioxane/20% 5xPBS (v/v, D<sub>20</sub>-fibrils), and raftlike liposomes (M-fibrils). W-fibrils were formed by incubating 50  $\mu\text{M}$   $\text{A}\beta$ -(1–40) in PBS for 1 w at  $37^{\circ}\text{C}$ . D<sub>20</sub>-fibrils and D-fibrils were produced by incubating 50  $\mu\text{M}$   $\text{A}\beta$ -(1–40) in corresponding solvent mixtures for 1 day at  $37^{\circ}\text{C}$  under an argon atmosphere. The absence of any oxidation products was confirmed by mass spectroscopy after dissolution with 95% dimethyl sulfoxide/4.5% water/0.5% trifluoroacetic acid. The fibrils were washed with PBS five times. M-fibrils were prepared by incubating 50  $\mu\text{M}$   $\text{A}\beta$ -(1–40) with raftlike SUVs composed of GM1/cholesterol/SM (4:3:3) ([GM1] = 50  $\mu\text{M}$ ) at  $37^{\circ}\text{C}$  for 3 days. The fibrils were washed with PBS three times. The concentration of  $\text{A}\beta$ -(1–40) in fibril suspensions was determined by reverse-phase HPLC after dissolution.

**Transmission Electron Microscopy (TEM).** TEM experiments were carried out by the Ultrastructure Research Institute, Hanaichi Co. Ltd. (Okazaki, Japan). Samples were spread on carbon-coated grids, negatively stained with uranyl acetate, and examined under a JEOL JEM-2000EX electron microscope with an acceleration voltage of 100 kV.

**FTIR.** Amyloid fibrils were collected by centrifugation (20000g, 10 min) and washed with water five times. Dry films of aggregates were prepared by spreading the pellets on a germanium attenuated total reflection (ATR) plate (80  $\times$  10  $\times$  4 mm) under a stream of nitrogen gas. The residual water was removed on  $\text{P}_2\text{O}_5$  under vacuum overnight. Trifluoroacetic acid, which gives absorption in the amide I region,<sup>23</sup> originating from  $\text{A}\beta$ -(1–40) was completely eliminated by this procedure because W-fibrils gave FTIR spectra indistinguishable to those formed by a HCl salt form of  $\text{A}\beta$ -(1–40) (data not shown). FTIR-ATR measurements were carried out on a BioRad FTS-3000MX spectrometer equipped with an Hg–Cd–Te detector and a PIKE horizontal ATR attachment. The total reflection number was 10 on the film side. The spectra were measured at a resolution of 2  $\text{cm}^{-1}$  and an angle of incidence of  $45^{\circ}$  and derived from 256 coadded interferograms with the Happ-Genzel apodization function. Subtraction of the gently sloping water vapor was carried out to improve the background prior to frequency measurement. For ATR correction, refractive indexes of 4.003 and 1.7 were used for germanium and protein, respectively.

**Surface Hydrophobicity.** For estimation of the hydrophobicity of amyloid fibrils, an ANS assay was carried out.<sup>24</sup> The amyloid sample (final  $\text{A}\beta$  concentration, 2.5  $\mu\text{M}$ ) was applied to a 5  $\mu\text{M}$  1-anilinonaphthalene-8-sulfonate (ANS) in PBS in a quartz cuvette and mixed by gentle stirring for 1 min. Fluorescence emission spectra were recorded at an excitation wavelength of 350 nm with a cuvette holder thermostated at  $25^{\circ}\text{C}$ .

**Cytotoxicity.** Human SH-SY5Y neuroblastoma cells were obtained from ECACC and cultured in D-MEM/F-12 containing 10% FBS, 100 U/mL penicillin, and 0.1 mg/mL streptomycin. After being plated at a density of 7000 cells/well onto a coverglass base, optical bottom 96-well microplate (Nunc, Roskilde, Denmark), the cells were incubated for more than 24 h at  $37^{\circ}\text{C}$  with 5%  $\text{CO}_2$  to allow cell attachment. The sample fibril suspension mixed with an equal volume of medium (final  $\text{A}\beta$ -(1–40) concentration, 25  $\mu\text{M}$ ) was applied

to each well and incubated for 24 h at 37 °C with 5% CO<sub>2</sub>. 100  $\mu$ L of calcein-AM (final concentration, 1  $\mu$ M) in PBS was gently added and incubated for 1 h at 37 °C. Calcein-AM (calcein tetraacetoxymethyl ester) is a membrane-permeable dye that is cleaved by intracellular esterases in living cells to produce the fluorophore calcein. Fluorescence was measured on a Wallac Envision (PerkinElmer, Waltham, MA). Linearity between the number of living cells and fluorescence intensity of calcein (excitation, 485 nm; emission, 535 nm) was confirmed. The fluorescence intensity of cells treated with only vehicle and the background fluorescence intensity of each well were defined as a positive control (viability; 100%) and as a negative control (viability; 0%), respectively. The statistical analysis was performed using ANOVA, and the significance was assessed against a positive control.

## RESULTS

**Polarity around A $\beta$ .** The polarity around A $\beta$  in raftlike liposomes was estimated by use of DAC-A $\beta$ -(1–40). Fluorescence spectra of DAC-A $\beta$ -(1–40) are sensitive to the surrounding polarity.<sup>7</sup> Figure 1 shows the wavelength of

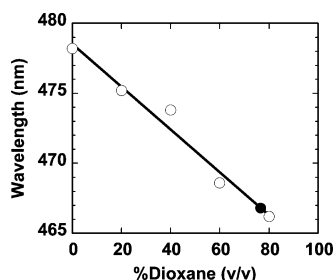


**Figure 1.** Dependence of fluorescence spectra of DAC-A $\beta$ -(1–40) on the surrounding polarity. Fluorescence spectra of 0.5  $\mu$ M DAC-A $\beta$ -(1–40) were measured in various 1,4-dioxane/PBS mixtures (open circles) as well as in the presence of raftlike SUVs composed of GM1/cholesterol/SM (4:3:3) ([GM1] = 50  $\mu$ M, closed circle) at 37 °C at an excitation wavelength of 415 nm. The salt concentrations were kept constant in all samples by use of differently concentrated PBS solutions. The wavelength of maximal intensity is plotted as a function of % dioxane (v/v). The experiments were performed in duplicate, and the errors were within 0.2 nm. The polarity around the protein in the liposomes corresponded to that of 77% dioxane.

maximal intensity as a function of solvent composition. The wavelength decreased almost linearly with the increase in the 1,4-dioxane content. The polarity around the protein in the liposomes corresponded to that of 77% (v/v) dioxane. Therefore, we used a 80% dioxane solution as a membrane mimic in the subsequent experiments. The polarity around DAC-A $\beta$ -(1–40) does not depend on the bound DAC-A $\beta$ -(1–40)/GM1 ratio because when a DAC-A $\beta$ -(1–40) solution was titrated with GM1-containing liposomes, each fluorescence spectrum could be described by a linear combination of the spectrum in buffer and the spectrum with excess liposomes (data not shown).

**Fibril Formation.** The formation of fibrils by A $\beta$ -(1–40) was monitored by the Th-T assay (Figure 2). In PBS, an increase in Th-T fluorescence was observed only after 2 days of incubation. In contrast, more hydrophobic media (GM1/cholesterol/SM (4:3:3) liposomes and 1,4-dioxane/5xPBS (80:20, v/v)) facilitated the formation of aggregates. The final level of ThT fluorescence in the presence of GM1-

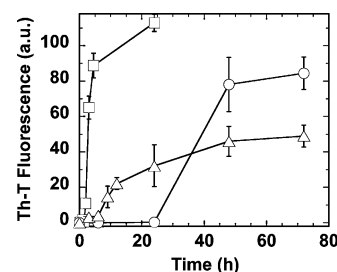


**Figure 2.** Fibril formation by A $\beta$ -(1–40) in various media. 50  $\mu$ M A $\beta$ -(1–40) were incubated in PBS (circles), 1,4-dioxane/5xPBS (80:20, v/v, squares), and raftlike SUVs composed of GM1/cholesterol/SM (4:3:3) ([GM1] = 50  $\mu$ M, triangles) at 37 °C under an argon atmosphere to avoid oxidation. Fibril formation was monitored by the Th-T assay. The experiments were performed in duplicate, and the error bars denote standard deviations.

liposomes was smaller than the other cases. It is underestimated because of the binding of positively charged ThT to negatively charged GM1. In the presence of both M-fibrils and liposomes, ThT molecules competitively bind to M-fibrils and liposomes. On the other hand, in blank samples containing only liposomes, all ThT molecules are available to GM1, giving larger background signals.

The morphology of the fibrils was observed by TEM (Figure 3). The aggregates that formed in 80% dioxane were typical

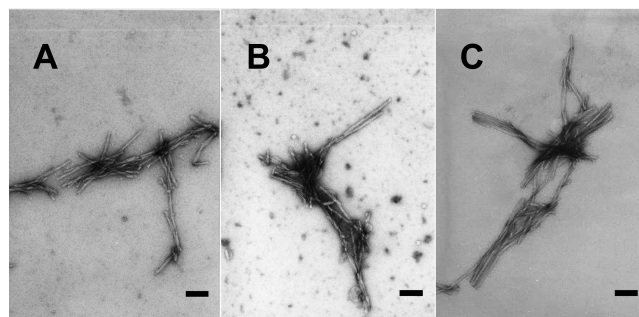


**Figure 3.** Negative stain TEM image of A $\beta$ -(1–40) fibrils formed in (A) buffer (W-fibrils), (B) raftlike SUVs (M-fibrils), and (C) 80% dioxane (D-fibrils). The scale bars represent 100 nm.

unbranched fibrils with a width of  $12.3 \pm 2.6$  nm (Figure 3C). Their morphology resembled that of M-fibrils with a width of  $11.8 \pm 0.4$  nm (Figure 3B) rather than that of W-fibrils with a width of  $7.9 \pm 0.6$  nm (Figure 3A). A similar width ( $\sim 8$  nm) was also reported for W-fibrils by other laboratories.<sup>25,26</sup>

Secondary structural features of A $\beta$ -(1–40) in 80% dioxane were estimated from the CD spectrum (Figure 4). The measurements were carried out at 15 °C to avoid aggregation of the protein. The absence of aggregation was confirmed by the Th-T assay (data not shown). The presence of a minima at around 220 nm indicates that the protein assumed a  $\beta$ -sheet-rich structure in this solvent mixture.

**FTIR.** The secondary structures of various amyloid fibrils was estimated by FTIR spectroscopy (Figure 5). All FTIR spectra exhibited intense bands at around  $1629\text{ cm}^{-1}$  (1629.8, 1629.2, 1628.3, and  $1628.5\text{ cm}^{-1}$  for W-, D<sub>20</sub>-, M-, and D-fibrils, respectively), indicating  $\beta$ -sheets are major conformations.<sup>27–29</sup> The wavenumber of maximal intensity decreased with solvent polarity. Minor bands at around  $1695\text{ cm}^{-1}$  were discernible in the spectra of amyloid fibrils formed in low-polarity environ-



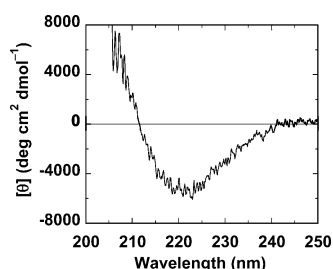


**Figure 4.** Secondary structure of A $\beta$ -(1–40) in 80% dioxane. The CD spectrum of 15  $\mu$ M A $\beta$ -(1–40) in 1,4-dioxane/5xPBS (80:20, v/v) was measured at 15 °C to avoid aggregation of the protein.

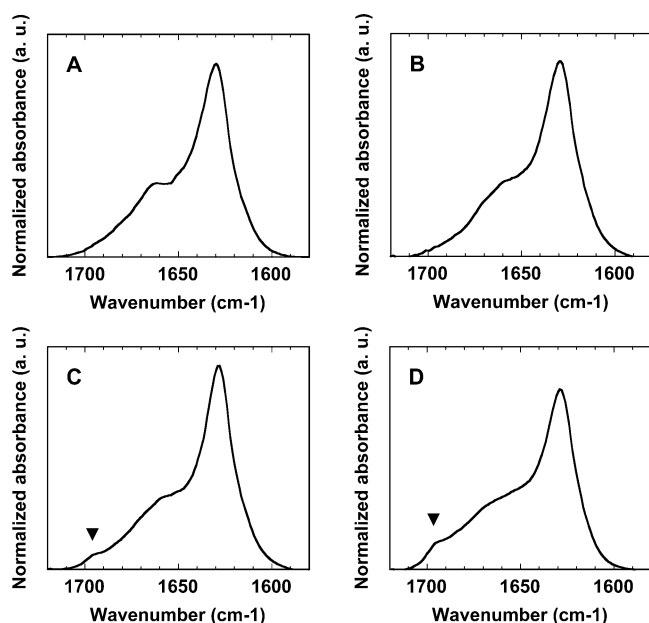


**Figure 5.** Secondary structure of various fibrils. FTIR spectra of A $\beta$ -(1–40) fibrils formed in (A) PBS (W-fibrils), (B) 20% 1,4-dioxane/80% 1.25xPBS (D<sub>20</sub>-fibrils), (C) raftlike liposomes (M-fibrils), and (D) 80% 1,4-dioxane/20% 5xPBS (D-fibrils) were measured by the ATR method. The arrowheads indicate minor peaks at around 1,695 cm<sup>–1</sup>. The spectra are normalized to have the same band area.

ments (M-fibrils and D-fibrils),<sup>a</sup> suggesting the presence of antiparallel  $\beta$ -sheets,<sup>27–29</sup> although this band may not be unique to antiparallel  $\beta$ -sheets.<sup>30</sup> The appearance of the minor peak in the spectrum of D-fibrils was due not to the presence of dioxane but to the low polarity because it was absent in the spectrum of fibrils formed in 20% dioxane (D<sub>20</sub>-fibrils). The appearance of the spectrum changed at around 60% dioxane (data not shown).

**Surface Hydrophobicity.** The surface hydrophobicity of various fibrils was estimated based on the binding of ANS. ANS is only weakly fluorescent in the aqueous phase; however, its fluorescence intensity increases with a blue shift in hydrophobic environments. Therefore, the dye is frequently used to monitor the presence of hydrophobic surfaces in proteins.<sup>24</sup> The addition of A $\beta$  fibrils to the ANS solution caused a significant increase in fluorescence accompanied by a blue-shift in the rank order D-fibrils  $\geq$  M-fibrils  $>$  W-fibrils (Figure 6).

**Cytotoxicity.** The cytotoxicity of various fibrils against human SH-SY5Y neuroblastoma cells was determined after a 24 h incubation with 25  $\mu$ M fibrils (Figure, 7). W-fibrils were

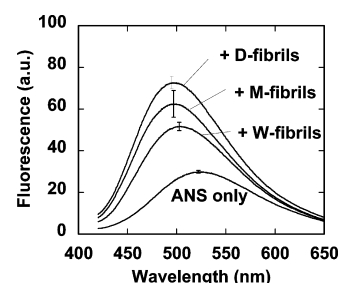


**Figure 6.** Surface hydrophobicity of various fibrils. Fluorescence spectra of 5  $\mu$ M ANS in PBS were measured in the absence and the presence of 2.5  $\mu$ M W-fibrils, M-fibrils, and D-fibrils at an excitation wavelength of 350 nm. The experiments were performed in duplicate, and the error bars denote standard deviations.

nontoxic, whereas M-fibrils and D-fibrils were equally toxic. The cell viability was reduced to  $\sim$ 50%.

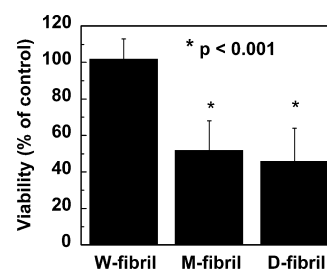


**Figure 7.** Cytotoxicity of various fibrils. The viability of human SH-SY5Y neuroblastoma cells in the presence of 25  $\mu$ M W-fibrils, M-fibrils, and D-fibrils was determined by the calcein-AM assay after a 24 h incubation at 37 °C (mean  $\pm$  standard deviation,  $n = 7$ –18;  $*p < 0.001$  against vehicle treatment).

## DISCUSSION

Membranes have been shown to facilitate the formation of amyloid fibrils by A $\beta$  as well as other amyloidogenic proteins.<sup>31</sup> However, the mechanism underlying membrane-induced formation of amyloid fibrils is not fully understood, although the local concentration of proteins and the induction of secondary structures have been proposed. Here, we found that low-polarity environments provided by membranes play an important role in not only the acceleration of fibrillization but also the formation of different types of fibrils from those formed in aqueous solution.

The polarity around A $\beta$ -(1–40) in raftlike membranes was close to that of 80% dioxane (Figure 1). FTIR<sup>32</sup> and NMR<sup>33</sup> studies suggested that A $\beta$ -(1–40) interacts with the sugar moieties of gangliosides and lies parallel to the surface of membranes. Thus, the estimated polarity is considered to represent that of the sugar region. It is noteworthy that both membrane and 80% dioxane environments promoted the fibril formation (Figure 2), even though local concentration effects are absent in the latter system. Low-polarity environments, in which the number of molecules capable of forming hydrogen bonds decreases compared to aqueous environments, facilitate the hydrogen bonding between A $\beta$ -(1–40) molecules rather than between A $\beta$ -(1–40) and environments, leading to the formation of secondary structures and eventually amyloid fibrils. A $\beta$ -(1–40) adopts a  $\beta$ -sheet-rich structure in both raftlike membranes<sup>7,8</sup> and 80% dioxane (Figure 4).

The wavenumber of maximal intensity of amide I band decreased with solvent polarity (Figure 5), indicating that amyloid fibrils formed in low-polarity environments have larger numbers of  $\beta$ -strands and/or stronger hydrogen bonds<sup>34,35</sup> than those formed in water. The latter interpretation is reasonable because hydrogen bonds are electrostatic in nature. In addition, they contain an antiparallel  $\beta$ -sheet structure, as suggested by the lower peak wavenumbers of the major amide I bands at around 1630  $\text{cm}^{-1}$  and the presence of minor bands at around 1695  $\text{cm}^{-1}$ , respectively (Figure 5). A theoretical study indicated that the 1695/1630 intensity ratio depends on the number of peptide chains and the number of peptide groups in the chain. For a single infinite antiparallel-chain pleated sheet, the ratio was estimated to be 0.085, and the observed value for polylysine was 0.099.<sup>36</sup> M- and D-fibrils exhibited 1695/1630 intensity ratios of 0.075 and 0.15, respectively. Both types of fibrils have significant antiparallel  $\beta$ -sheet contents, although they are not identical. Heterogeneous membranes and homogeneous solutions do not give identical environments, or M- and D-fibrils are mixtures of fibrils with parallel and antiparallel  $\beta$ -sheets in different ratios because both types of  $\beta$ -sheets appear to be very similar in thermodynamic stability.<sup>4</sup> In any case, it is clear that polarity affects the major type of fibrils; fibrils containing parallel  $\beta$ -sheets were formed in more polar 20% dioxane (Figure 5). The two dioxane-containing solutions having different polarity do not significantly differ in other physicochemical properties, such as viscosity (0.711 cP in 20% dioxane vs 0.885 cP in 80% dioxane at 40 °C, close to our experimental temperature). Such a small difference in viscosity will slightly affect the kinetics of peptide aggregation but not the type of fibrils. Indeed, water at 25 °C has a similar viscosity (0.890 cP) to 80% dioxane at 40 °C, but parallel-type fibrils are formed in water at 25 °C.

Short A $\beta$  fragments<sup>37,38</sup> as well as the Iowa A $\beta$ -(1–40) mutant<sup>39</sup> have been reported to form amyloid fibrils composed of antiparallel  $\beta$ -sheets. Oligomers of A $\beta$ -(1–40)<sup>40,41</sup> and A $\beta$ -(1–42)<sup>42</sup> have also been suggested to have an antiparallel  $\beta$ -sheet structure. The formation of in-register parallel  $\beta$ -sheets is unfavorable in low-polarity environments because electrostatic repulsion between charged amino acid side chains in adjacent  $\beta$ -strands is manifested in media of low dielectric constant. Furthermore, an antiparallel orientation of macrodipoles of helices, precursors of  $\beta$ -sheets,<sup>8</sup> is also preferable in media of low dielectric constant.

The surfaces of M-fibrils and D-fibrils were more hydrophobic than that of W-fibrils (Figure 6). W-fibrils have been proposed to have in-register parallel  $\beta$ -sheet structures in which hydrophobic amino acids are effectively sequestered from water.<sup>10,11</sup> In contrast, it appears to be difficult for M-fibrils and D-fibrils possessing antiparallel  $\beta$ -sheets to completely bury nonpolar amino acids inside the fibrils. Both the extent of surface hydrophobicity<sup>43</sup> and the presence of antiparallel  $\beta$ -sheets<sup>44,45</sup> have been reported to correlate closely with the cytotoxicity of various amyloid fibrils and soluble oligomers.

In summary, ganglioside clusters mediate the formation of toxic amyloid fibrils of A $\beta$ -(1–40) with an antiparallel  $\beta$ -sheet structure by providing less polar environments. The precise structure of the fibrils is under investigation by use of isotope-edited FTIR and solid-state NMR.

## AUTHOR INFORMATION

### Corresponding Author

\*Phone +81 75-753-4521; Fax +81 75-753-4578; e-mail mkatsumi@pharm.kyoto-u.ac.jp.

### Funding

This work was supported in part by The Research Funding for Longevity Sciences (22-14) from National Center for Geriatrics and Gerontology (NCGG), Japan.

### Notes

The authors declare no competing financial interest.

## ABBREVIATIONS

A $\beta$ , amyloid  $\beta$ -protein; AD, Alzheimer's disease; ANS, 1-anilinonaphthalene-8-sulfonate; ATR, attenuated total reflection; calcein-AM, calcein tetraacetoxymethyl ester; CD, circular dichroism; FTIR, Fourier-transform infrared; GM1, monosialoganglioside GM1; D-fibrils, A $\beta$  fibrils formed in 80% 1,4-dioxane/20% 5xPBS (v/v); D<sub>20</sub>-fibrils, A $\beta$  fibrils formed in 20% 1,4-dioxane/80% 1.25xPBS (v/v); DAC-A $\beta$ -(1–40), A $\beta$ -(1–40) labeled with the 7-diethylaminocoumarin-3-carbonyl group at its N-terminus; M-fibrils, A $\beta$  fibrils formed in raftlike liposomes; PBS, phosphate-buffered saline; SM, N-acyl-D-sphingosine-1-phosphocholine from bovine brain; SUV, small unilamellar vesicle; ThT, thioflavin T; W-fibrils, A $\beta$  fibrils formed in PBS.

## ADDITIONAL NOTE

<sup>a</sup>FTIR spectra of proteins are often measured in D<sub>2</sub>O to avoid spectral contributions from water. We also measured FTIR spectra of M-fibrils prepared in D<sub>2</sub>O-based PBS. However, their spectra were very similar to those of W-fibrils prepared in D<sub>2</sub>O-based PBS, suggesting that M-fibrils and W-fibrils are very similar in thermodynamic stability and mutually convertible following subtle changes in conditions, such as the deuteration of water, which is known to affect the stability of proteins.<sup>46</sup> Contributions from bound water, if any, were negligible because the samples were extensively dried up on P<sub>2</sub>O<sub>5</sub> and the spectra were reproducible.

## REFERENCES

- (1) Selkoe, D. J. (1994) Cell biology of the amyloid  $\beta$ -protein precursor and the mechanism of Alzheimer's disease. *Annu. Rev. Cell Biol.* 10, 373–403.
- (2) Hardy, J., and Selkoe, D. J. (2002) The amyloid hypothesis of Alzheimer's disease: Progress and problems on the road to therapeutics. *Science* 297, 353–356.
- (3) Matsuzaki, K. (2007) Physicochemical interactions of amyloid  $\beta$ -peptide with lipid bilayers. *Biochim. Biophys. Acta* 1768, 1935–1942.
- (4) Matsuzaki, K., Kato, K., and Yanagisawa, K. (2010) A $\beta$  polymerization through interaction with membrane gangliosides. *Biochim. Biophys. Acta* 1801, 868–877.
- (5) Yanagisawa, K. (2007) Role of gangliosides in Alzheimer's disease. *Biochim. Biophys. Acta* 1768, 1943–1951.
- (6) Ariga, T., McDonald, M. P., and Yu, R. K. (2008) Role of ganglioside metabolism in the pathogenesis of Alzheimer's disease—a review. *J. Lipid Res.* 49, 1157–1175.
- (7) Kakio, A., Nishimoto, S., Yanagisawa, K., Kozutsumi, Y., and Matsuzaki, K. (2001) Cholesterol-dependent formation of GM1 ganglioside-bound amyloid  $\beta$ -protein, an endogenous seed for Alzheimer amyloid. *J. Biol. Chem.* 276, 24985–24990.
- (8) Ikeda, K., Yamaguchi, T., Fukunaga, S., Hoshino, M., and Matsuzaki, K. (2010) Mechanism of amyloid  $\beta$ -protein aggregation mediated by GM1 ganglioside clusters. *Biochemistry* 50, 6433–6440.

- (9) Okada, T., Ikeda, K., Wakabayashi, M., Ogawa, M., and Matsuzaki, K. (2008) Formation of toxic A $\beta$ (1–40) fibrils on GM1 ganglioside-containing membranes mimicking lipid rafts: Polymorphisms in A $\beta$ (1–40) fibrils. *J. Mol. Biol.* 382, 1066–1074.
- (10) Antzakin, O. N., Balbach, J. J., Leapman, R. D., Rizzo, N. W., Reed, J., and Tycko, R. (2000) Multiple quantum solid-state NMR indicates a parallel, not antiparallel, organization of  $\beta$ -sheets in Alzheimer's  $\beta$ -amyloid fibrils. *Proc. Natl. Acad. Sci. U. S. A.* 97, 13045–13050.
- (11) Petkova, A. T., Ishii, Y., Balbach, J. J., Antzakin, O. N., Leapman, R. D., Delaglio, F., and Tycko, R. (2002) A structural model for Alzheimer's  $\beta$ -amyloid fibrils based on experimental constraints from solid state NMR. *Proc. Natl. Acad. Sci. U. S. A.* 99, 16742–16747.
- (12) Lee, E. K., Hwang, J. H., Shin, D. Y., Kim, D. I., and Yoo, Y. J. (2005) Production of recombinant amyloid- $\beta$  peptide 42 as an ubiquitin extension. *Protein Expression Purif.* 40, 183–189.
- (13) Yamaguchi, T., Yagi, H., Goto, Y., Matsuzaki, K., and Hoshino, M. (2010) A disulfide-linked amyloid- $\beta$  peptide dimer forms a protofibril-like oligomer through a distinct pathway from amyloid fibril formation. *Biochemistry* 49, 7100–7107.
- (14) Okada, T., Wakabayashi, M., Ikeda, K., and Matsuzaki, K. (2007) Formation of toxic fibrils of Alzheimer's amyloid  $\beta$ -protein-(1–40) by monosialoganglioside GM1, a neuronal membrane component. *J. Mol. Biol.* 371, 481–489.
- (15) Kakio, A., Nishimoto, S., Yanagisawa, K., Kozutsumi, Y., and Matsuzaki, K. (2002) Interactions of amyloid  $\beta$ -protein with various gangliosides in raft-like membranes: Importance of GM1 ganglioside-bound form as an endogenous seed for Alzheimer amyloid. *Biochemistry* 41, 7385–7390.
- (16) Svennerholm, L. (1957) Quantitative estimation of sialic acids. II. A colorimetric resorcinol-hydrochloric acid method. *Biochim. Biophys. Acta* 24, 604–611.
- (17) Bartlett, G. R. (1959) Phosphorus assay in column chromatography. *J. Biol. Chem.* 234, 466–468.
- (18) Matsuzaki, K., Noguchi, T., Wakabayashi, M., Ikeda, K., Okada, T., Ohashi, Y., Hoshino, M., and Naiki, H. (2007) Inhibitors of amyloid  $\beta$ -protein aggregation mediated by GM1-containing raft-like membranes. *Biochim. Biophys. Acta* 1768, 122–130.
- (19) Yamamoto, N., Matsuzaki, K., and Yanagisawa, K. (2005) Cross-seeding of wild-type and hereditary variant type amyloid  $\beta$ -proteins in the presence of gangliosides. *J. Neurochem.* 95, 1167–1176.
- (20) Naiki, H., and Gejyo, F. (1999) Kinetic analysis of amyloid fibril formation. *Methods Enzymol.* 309, 305–318.
- (21) LeVine, I. H. (1993) Thioflavine T interaction with synthetic Alzheimer's disease  $\beta$ -amyloid peptides: Detection of amyloid aggregation in solution. *Protein Sci.* 2, 404–410.
- (22) Takakuwa, T., Konno, T., and Meguro, H. (1985) A new standard substance for calibration of circular dichroism: Ammonium *d*-10-camphorsulfonate. *Anal. Sci.* 1, 215–218.
- (23) Surewicz, W. K., and Mantsch, H. H. (1989) The conformation of dynorphin A-(1–13) in aqueous solution as studied by Fourier transform infrared spectroscopy. *J. Mol. Struct.* 214, 143–147.
- (24) Turner, D. C., and Brand, L. (1968) Quantitative estimation of protein binding site polarity. Fluorescence of *N*-arylaminonaphthalenesulfonates. *Biochemistry* 7, 3381–3390.
- (25) Maji, S. K., Amsden, J. J., Rothschild, K. J., Condron, M. M., and Teplow, D. B. (2005) Conformational dynamics of amyloid  $\beta$ -protein assembly probed using intrinsic fluorescence. *Biochemistry* 44, 13365–13376.
- (26) Paravatsu, A. K., Leapman, R. D., Yau, W.-M., and Tycko, R. (2008) Molecular structural basis for polymorphism in Alzheimer's  $\beta$ -amyloid fibrils. *Proc. Natl. Acad. Sci. U. S. A.* 105, 18349–18354.
- (27) Miyazawa, T. (1960) Perturbation treatment of the characteristic vibrations of polypeptide chains in various configurations. *J. Chem. Phys.* 32, 1647–1652.
- (28) Miyazawa, T., and Blout, E. R. (1961) The infrared spectra of polypeptides in various conformations: Amide I and II bands. *J. Am. Chem. Soc.* 83, 712–719.
- (29) Jackson, M., and Mantsch, H. H. (1995) The use and misuse of FTIR spectroscopy in the determination of protein structure. *Crit. Rev. Biochem. Mol. Biol.* 30, 95–120.
- (30) Khurana, R., and Fink, A. L. (2000) Do parallel  $\beta$ -helix proteins have a unique Fourier transform infrared spectrum? *Biophys. J.* 78, 994–1000.
- (31) Butterfield, S. M., and Lashuel, H. A. (2010) Amyloidogenic protein-membrane interactions: Mechanistic insight from model systems. *Angew. Chem., Int. Ed.* 49, 5628–5654.
- (32) Matsuzaki, K., and Horikiri, T. (1999) Interactions of amyloid  $\beta$ -peptide (1–40) with ganglioside-containing membranes. *Biochemistry* 38, 4137–4142.
- (33) Utsumi, M., Yamaguchi, Y., Sasakawa, H., Yamamoto, N., Yanagisawa, K., and Kato, K. (2008) Up-and-down topological mode of amyloid  $\beta$ -peptide lying on hydrophilic/hydrophobic interface of ganglioside clusters. *Glycoconjugate. J.* 26, 999–1006.
- (34) Kubelka, J., and Keiderling, T. A. (2001) Differentiation of  $\beta$ -sheet-forming structures: Ab initio-based simulations of IR absorption and vibrational CD for model peptide and protein  $\beta$ -sheets. *J. Am. Chem. Soc.* 123, 12048–12058.
- (35) Zandomeni, G., Krebs, M. R., McCammon, M. G., and Fändrich, M. (2004) FTIR reveals structural differences between native  $\beta$ -sheet proteins and amyloid fibrils. *Protein Sci.* 13, 3314–3321.
- (36) Chirgadze, Y. N., and Nevskaya, N. A. (1976) Infrared spectra and resonance interaction of amide-I vibration of the parallel-chain pleated sheet. *Biopolymers* 15, 627–636.
- (37) Lansbury, P. T. J., Costa, P. R., Griffiths, J. M., Simon, E. J., Auger, M., Halverson, K. J., Kocisko, D. A., Hendsch, Z. S., Ashburn, T. T., Spencer, R. G., Tidor, B., and Griffin, R. G. (1995) Structural model for the  $\beta$ -amyloid fibril based on interstrand alignment of an antiparallel-sheet comprising a C-terminal peptide. *Nat. Struct. Biol.* 2, 990–998.
- (38) Balbach, J. J., Ishii, Y., Antzakin, O. N., Leapman, R. D., Rizzo, N. W., Dyda, F., Reed, J., and Tycko, R. (2000) Amyloid fibril formation by A $\beta$  16–22, a seven-residue fragment of the Alzheimer's  $\beta$ -amyloid peptide, and structural characterization by solid state NMR. *Biochemistry* 39, 13748–13759.
- (39) Qiang, W., Yau, W.-M., Luo, Y., Mattson, M. P., and Tycko, R. (2012) Antiparallel  $\beta$ -sheet architecture in Iowa-mutant  $\beta$ -amyloid fibrils. *Proc. Natl. Acad. Sci. U. S. A.* 109, 4443–4448.
- (40) Habicht, G., Haupt, C., Friedrich, R. P., Hortschansky, P., Sachse, C., Meinhardt, J., Wieligmann, K., Gellermann, G. P., Brodhun, M., Götz, J., Halbherr, K. J., Röcken, C., Horn, U., and Fändrich, M. (2007) Directed selection of a conformational antibody domain that prevents mature amyloid fibril formation by stabilizing A $\beta$  protofibrils. *Proc. Natl. Acad. Sci. U. S. A.* 104, 19232–19237.
- (41) Sarroukh, R., Cerf, E., Derclay, S., Dufrène, Y. F., Goormaghtigh, E., Ruysschaert, J. M., and Raussens, V. (2011) Transformation of amyloid  $\beta$ (1–40) oligomers into fibrils is characterized by a major change in secondary structure. *Life Sci.* 68, 1429–1438.
- (42) Cerf, E., Sarroukh, R., Tamamizu-Kato, S., Breydo, L., Derclay, S., Dufrène, Y. F., Narayanaswami, V., Goormaghtigh, E., Ruysschaert, J. M., and Raussens, V. (2009) Antiparallel  $\beta$ -sheet: A signature structure of the oligomeric amyloid  $\beta$ -peptide. *Biochem. J.* 421, 415–423.
- (43) Bolognesi, B., Kumita, J. R., Barros, T. P., Esbjörner, E. K., Luheshi, L. M., Crowther, D. C., Wilson, M. R., Dobson, C. M., Favrin, G., and Yerbury, J. J. (2010) ANS binding reveals common features of cytotoxic amyloid species. *ACS Chem. Biol.* 5, 735–740.
- (44) Berthelot, K., Ta, H. P., Géan, J., Lecomte, S., and Cullin, C. (2011) In vivo and in vitro analyses of toxic mutants of HET-s: FTIR antiparallel signature correlates with amyloid toxicity. *J. Mol. Biol.* 412, 137–152.
- (45) Stroud, J. C., Liu, C., Teng, P. K., and Eisenberg, D. (2012) Toxic fibrillar oligomers of amyloid- $\beta$  have cross- $\beta$  structure. *Proc. Natl. Acad. Sci. U. S. A.* 109, 7717–7722.

(46) Makhatadze, G. I., Clore, G. M., and Gronenborn, A. M. (1995) Solvent isotope effect and protein stability. *Nat. Struct. Biol.* 2, 852–855.